HHS Public Access

Author manuscript

Nanomedicine. Author manuscript; available in PMC 2021 January 01.

Published in final edited form as:

Nanomedicine. 2020 January ; 23: 102115. doi:10.1016/j.nano.2019.102115.

Nonviral Polymeric Nanoparticles for Gene Therapy in Pediatric CNS Malignancies

John Choi[1,*], **Yuan Rui**[2,3,*], **Jayoung Kim**[2,3,*], **Noah Gorelick**[1], **David R. Wilson**[2,3], **Kristen Kozielski**[2,3], **Antonella Mangraviti**[1], **Eric Sankey**[1], **Henry Brem**[1,2,4], **Betty Tyler**[1], **Jordan J. Green**[1,2,3,4,5,6,#], **Eric M. Jackson**[1,#]

[1]Department of Neurosurgery, Johns Hopkins University School of Medicine

[2]Department of Biomedical Engineering, Johns Hopkins University School of Medicine

[3]The Institute for Nanobiotechnology and the Translational Tissue Engineering Center, Johns Hopkins University School of Medicine

[4]Departments of Ophthalmology and Oncology, Johns Hopkins University School of Medicine

[5]Departments of Materials Science & Engineering and Chemical & Biomolecular Engineering, Johns Hopkins University

[6]Bloomberg~Kimmel Institute for Cancer Immunotherapy, Johns Hopkins University School of Medicine.

Abstract

Together, medulloblastoma (MB) and atypical teratoid/rhabdoid tumors (AT/RT) represent two of the most prevalent pediatric brain malignancies. Current treatment involves radiation, which has high risks of developmental sequelae for patients under the age of three. New safer and more effective treatment modalities are needed. Cancer gene therapy is a promising alternative, but there are challenges with using viruses in pediatric patients. We developed a library of poly(beta-amino ester) (PBAE) nanoparticles and evaluated their efficacy for plasmid delivery of a suicide gene therapy to pediatric brain cancer models—specifically herpes simplex virus type I thymidine kinase (HSVtk), which results in controlled apoptosis of transfected cells. *In vivo*, PBAE-HSVtk treated groups had a greater median overall survival in mice implanted with AT/RT ($p=0.0083$ *v.s. control*) and MB ($p<0.0001$ *vs. control*). Our data provides proof of principle for using biodegradable PBAE nanoparticles as a safe and effective nanomedicine for treating pediatric CNS malignancies.

Graphical Abstract

[#]Correspondence should be addressed to: *Eric M. Jackson, M.D.,* Department of Pediatric Neurosurgery, 600 N. Wolfe St., Phipps Building 521, Baltimore, MD 21287, USA. ejacks34@jhmi.edu. (410) 955-7740 *Jordan J Green, Ph.D.,* Department of Biomedical Engineering, 400 N. Broadway, Smith Building 5017, Baltimore, MD 21231, USA. green@jhu.edu. (410) 614-9113.

[*]These authors contributed equally

There are no conflict of interests as pertinent to the development of manuscript.

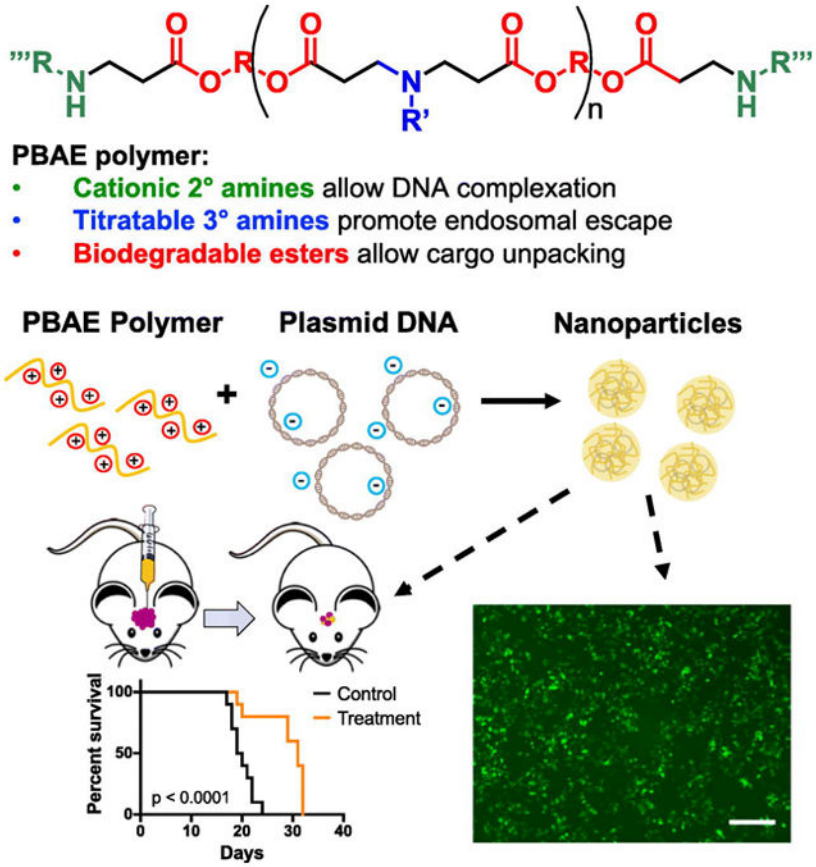

Poly(beta-amino ester)s (PBAEs) are biodegradable, cationic polymers that can self-assemble into nanoparticles with nucleic acids. Nanoparticles formulated with plasmid DNA for intracellular gene delivery to pediatric brain cancer cells enabled >50% transfection in both cell lines tested. *In vivo* intracranial administration of nanoparticles carrying the HSVtk suicide gene to mice bearing orthotopic tumor xenografts significantly enhanced survival.

Keywords

Pediatrics; Cancer; Medulloblastoma; Atypical teratoid/rhabdoid tumor; Poly(Beta-Amino Ester) nanoparticle

Background

Malignant CNS tumors are the most common solid tumor in children.[1] Of those, medulloblastoma (MB) accounts for about 20 percent of all pediatric CNS tumors.[2] However, in children younger than 6 months of age, atypical teratoid/rhabdoid tumors (AT/RT) are the most common malignant central CNS tumor.[3] Historically, it has been difficult to distinguish these two cancers based on radiology alone, particularly since both occur almost exclusively in the cerebellum. Current diagnostic criteria of AT/RT require immunohistochemistry (IHC) characterization of SMARCB1/INI1 or evidence of SMARCA4/BRG1 deletion and/or mutation of 22q11.2 to distinguish it from MB.[4-5]

Of note, the prevalence of these two tumors in pediatric populations younger than three years of age complicates treatment; chemotherapy is often used to delay or avoid radiotherapy in infantile medulloblastoma,[6] while lack of effective therapies for AT/RT often requires use of initial radiotherapy for treatment despite the risk of neurologic sequelae that arises from early childhood radiation.[7] Even with radiation and surgery, patients with AT/RT report a dismal prognosis with median overall survival of 1 year.[8-9] Therefore, expansion of new treatment modalities for these malignancies is imperative for improving mortality outcomes in these pediatric populations.

We recently explored the potential of a new nanomedicine, poly(beta-amino ester) (PBAE) nanoparticles containing plasmid DNA encoding the suicide gene herpes simplex virus I thymidine kinase (HSVtk), as a gene therapy for treating adult glioma.[10] We found that in a preclinical glioma rat study, the nanoparticles could spread through the tumor and there was a significant increase in median overall survival *in vivo*.[10] The well-characterized safety profile and effectiveness of PBAE nanoparticles for gene delivery—along with the ability to engineer these particles to avoid unwanted immunogenic risks—make them a promising candidate for pediatric malignancies,[11-15] although this direction has not been previously investigated. Of note, there has been a recent emergence of interest in using nanoparticles for gene delivery in pediatric malignancies, with cationic lipid-polymer hybrid nanoparticles (CLPNs) showing *in vivo* transfection efficacy in childhood rhabdomyosarcoma.[16]

Specifically, PBAEs are a class of polymeric nanoparticles that can be engineered to contain primary, secondary, and tertiary amines with hydrolytically cleavable ester bonds that allow for effective DNA binding and encapsulation, endocytosis within the host cell, subsequent endosomal escape, and intracellular DNA release for transcription and translation of the exogenous gene of interest.[17] Previous studies have shown that PBAEs can be safe and effective DNA delivery vectors both *in vitro* across multiple tissue types as well as *in vivo* in retinal and brain tissue.[11-13] Furthermore, PBAE polymers degrade quickly under physiological conditions, thereby minimizing nanoparticle cytotoxicity as well as maximizing successful delivery of nucleic acids.[18] Notably, PBAEs also demonstrate biomaterial-mediated cell type specificity, and are able to selectively transfect tumor tissue over healthy tissue in the brain [13, 19] and liver. [20-21]

Additionally, convection-enhanced delivery (CED) has been shown to be an effective method for locally delivering PBAEs to tumor sites *in vivo* by maintaining a pressure gradient that enhances diffusion of the particles throughout the tumor mass.[22] In a previous study, we demonstrated increased distribution of particles using CED *in vivo*.[10] Therefore, this study aims to investigate the efficacy of PBAE nanoparticles for intracellular delivery of nucleic acids such as plasmid DNA encoding HSVtk to show proof of principle that these polymeric nanoparticles can be used as a safe and effective method for treatment delivery in MB and AT/RT.

Methods

Materials

Small molecule monomers: 1,4-butanediol diacrylate (B4; CAS 1070-70-8), 3-amino-1-propanol (S3, CAS 156-87-6), 4-amino-1-butanol (S4, CAS 13325-10-05), 5-amino-1-pentanol (S5, CAS 2508-29-4), and 1-(3-aminopropyl)-4-methylpiperazine (E7, CAS 4572-031) were purchased from Alfa Aesar (Ward Hill, MA, USA); 1,5-pentanediol diacrylate (B5, CAS 36840-85-4) was purchased from Dajac Laboratories (Feasterville-Trevose, PA, USA); 2-(3-aminopropylamino)ethanol (E6; CAS 4461-39-6) was purchased from Sigma Aldrich (St. Louis, MO, USA). Lipofectamine™ 2000 and Lipofectamine 3000™ were purchased from ThermoFisher (Waltham, MA, USA). 25 kD branched poly(ethylenimine) was purchased from Sigma Aldrich (St. Louis, MO, USA). The pEGFP-N1 plasmid (GFP) was purchased from Elim Biopharmaceuticals (Hayward, CA, USA) and the herpes simplex virus type 1-derived thymidine kinase (HSVtk) gene was cloned into the pcDNA3.1 vector; both plasmids were amplified by Aldeveron (Fargo, ND, USA). For cell staining in *in vitro* cell killing assays, Hoechst 33342 and propidium iodide were purchased from Invitrogen (Carlsbad, CA, USA). CellTiter 96 AQ_{ueous} One MTS assay was purchased from Promega (Madison, Wisconsin, USA). Ganciclovir was purchased from Invivogen (Carlsbad, CA, USA).

Polymer Synthesis and Characterization

B and S monomers were reacted at a molar ratio of 1.1:1 at 90°C with stirring overnight to form acrylate-terminated base polymers. Base polymers were then dissolved in anhydrous THF at 167 mg/mL and added to end-capping E monomers (0.5 M in THF) at a 3:2 volume ratio and allowed to react at room temperature with stirring for 1 hour, at which time polymers were washed twice in diethyl ether to remove unreacted monomers and oligomers. Solvents were removed in a vacuum desiccant chamber for 2 days, at which point polymers were dissolved in DMSO at 100 mg/mL, and single-use aliquots were stored at −20°C with desiccant.

Nuclear magnetic resonance spectroscopy (NMR) was used to characterize polymer structure via ^{1}H NMR in $CDCl_3$ (Bruker 500 MHz) and analyzed using TopSpin 3.5 software (Billerica, MA, USA). Gel permeation chromatography (Waters, Milford, MA) measurements were performed to measure polymer molecular weight and polydispersity. Polymers were dissolved in BHT-stabilized tetrahydrofuran and 5% DMSO and 1% piperidine, filtered through a 0.2 μm PTFE filter and measured against linear polystyrene standards.

Nanoparticle Characterization

Nanoparticles were prepared in the same manner as for transfections and diluted in 150 mM PBS to determine nanoparticle characteristics in neutral isotonic buffer. Hydrodynamic diameter was measured via dynamic light scattering at 1:6 dilution in PBS using a Malvern Zetasizer NanoZS (Malvern Panalytical, Malvern, UK). Zeta potential was measured via electrophoretic light scattering on the same Malvern Zetasizer. For characterization of lyophilized nanoparticles, nanoparticles were first resuspended in water following the same

procedure as *in vivo* experiments and then diluted in PBS to the same polymer concentration as freshly prepared nanoparticles before measurement using dynamic light scattering. Transmission electron microscopy (TEM) images were acquired using a Philips CM120 (Philips Research, Cambridge, MA, USA). Nanoparticles were prepared at a polymer concentration of 1.8 mg/mL in 25 mM sodium acetate buffer (NaAc), and 30 μL were added to 400-square mesh carbon-coated TEM grids and allowed to dry for 20 min, at which point grids were rinsed with ultrapure water and allowed to fully dry before imaging.

Cell Culture

Human BT-12 atypical teratoid/rhabdoid tumor (AT/RT) cells (obtained from C. Eberhart's laboratory, Johns Hopkins University, Baltimore, MD, USA) were cultured in Dulbecco's Modified Eagle Media (DMEM; ThermoFisher, Waltham, MA, USA) supplemented with 10% FBS and 1% penicillin/streptomycin. D425 group 3 medulloblastoma cells (obtained from C. Eberhart's laboratory, Johns Hopkins University, Baltimore, MD, USA) were cultured in Minimum Essential Medium (MEM; ThermoFisher, Waltham, MA, USA) supplemented Within non-essential amino acids, 10% FBS, and 1% penicillin/streptomycin.

Transfection

BT-12 cells were seeded onto 96 well tissue culture plates at a density of 15,000 cells per well in 100 μL complete medium and allowed to adhere for 48 hours before transfection. D425 cells were seeded at a density of 15,000 cells per well 24 hours prior to transfection (transfection was done with cells in suspension as D425s did not adhere to tissue culture plates). To form nanoparticles, plasmid DNA and polymer were first dissolved separately in 25 mM NaAc buffer (pH 5) at the desired concentration and then mixed together at a 1:1 volume ratio. Nanoparticles were allowed to self-assemble for 10 minutes at room temperature before being added to cells. Nanoparticles were incubated with cells for 2 hours, at which time cells were replenished with fresh complete medium. To test the transfection efficacy of lyophilized nanoparticles, nanoparticles were first resuspended in water and then added to cells in complete cell culture medium to achieve a final DNA dose matching that delivered by freshly prepared nanoparticles (600 ng DNA per well). Nanoparticle-mediated cytotoxicity was assessed 24 hours post-transfection using CellTiter 96 AQ_{ueous} One MTS cell proliferation assay (Promega, Madison, Wisconsin, USA) following manufacturer's instructions. Transfection efficacy was assessed 48 hours post-transfection via flow cytometry using a BD Accuri C6 flow cytometer (BD Biosciences, Franklin Lakes, NJ, USA). N = 4 +/− SEM.

Transfections using commercially-available non-viral transfection reagents Lipofectamine 2000™ and Lipofectamine 3000™(ThermoFisher, Waltham, MA, USA) were performed according to manufacturer instructions.

Nanoparticle Uptake and Endocytosis Pathway Inhibition

Cellular uptake of nanoparticles was measured using nanoparticles encapsulating 20% Cy5-labeled DNA (prepared using previously published protocols[23]) and 80% unlabeled plasmid DNA. Nanoparticles were prepared and added to cells in the same manner as for *in vitro* transfections described above. After 2 h incubation with cells, nanoparticles were removed

and cells were washed once with PBS before being prepared for flow cytometry experiments. Nanoparticle uptake was quantified both as percentage of cells with Cy5 fluorescence after gating against untreated cells as well as by using the geometric mean Cy5 fluorescence intensity normalized to that of untreated cells.

To investigate the relationship between polymer structure and endocytosis pathways leading to nanoparticle uptake and transfection, BT-12 cells were pre-treated with small molecule drugs inhibiting specific endocytosis pathways for 1 h prior to the addition of nanoparticles. Endocytosis inhibitors were used at the highest concentrations that did not lead to significant levels of inhibitor-mediated cytotoxicity and are as follows: 16 μg/mL chlorpromazine, 1.5 mg/mL methyl-β-cyclodextrin, 36 μg/mL genistein, and 3,5 μg/mL cytochalasin-D. After 1 h pre-incubation with inhibitors, nanoparticles were added to cells and incubated for an additional 2 h, after which cells were prepared for flow cytometry for uptake experiments or replenished with fresh complete media for transfection experiments.

In Vitro HSVtk Cell Killing Assay

For HSVtk cell killing assays, transfection was performed as described above using HSVtk and GFP plasmids, respectively. Ganciclovir (Invivogen, San Diego, CA, USA) was resuspended in PBS at 5 mg/mL following manufacturer's instructions and diluted to desired concentrations using complete cell culture media. On days 1, 3, and 5 after transfection, cells were treated with fresh ganciclovir-containing media. On day 7 post-transfection, cells were stained with Hoechst 33342 nuclear stain (1:1000 dilution) and propidium iodide (1:500 dilution) for 20 minutes and imaged and analyzed using Cellomics Arrayscan VTI with live cell imaging module. Cell killing was calculated by normalizing live cell numbers in treated wells to those in untreated wells.

Tumor Implantation

All animal work was done in strict adherence of the policies and guidelines of the Johns Hopkins University Animal Care and Use Committee (ACUC Mouse Protocol Mo17M185). For intracranial tumor implantation, 6-8 week old male athymic nude mice (Charles River, Wilmington, MA, USA) were anesthetized using a Ketamine (100 mg/kg)/Xylazine (10 mg/kg) cocktail and mounted on a stereotactic frame. A rostro-caudal incision was made with a scalpel, the skin was spread apart, the surface of the skull was exposed and cleaned with 100% ethanol, and a small hole was made using an electric drill in the skull 2 mm posterior to the coronal suture and 2 mm lateral to the sagittal suture. Stainless steel cannulas (C212SG PlasticsOne®, Roanoke, VA, USA) were implanted into the hole in the skull. 5e5 BT-12 cells and 1.25e5 D425 cells were respectively implanted into mouse brains into the left striatum through cannulas.

In Vivo Nanoparticle Administration

Xenograft tumors were allowed to form for 10 days for BT-12 and 7 days for D425, at which time nanoparticle administration began. For *in vivo* injections, nanoparticles were lyophilized after initial formation as described previously.[24] Briefly, nanoparticles were formulated at *in vitro* optimized polymer-to-DNA w/w ratio but with the total polymer concentration at 5 mg/mL; sucrose was added at a final concentration of 30 mg/mL as a

cryoprotectant. Lyophilized nanoparticles were resuspended in sterile water at a final isotonic sucrose concentration of 100 mg/mL immediately before intracranial administration. Mice were anesthetized, and the original incision was opened. Convection-enhanced delivery (CED) was performed using a 26-gauge needle stereotactically placed at a depth of 3 mm and an UltraMicroPump (UMP3) with SYS-Micro4 Controller (World Precision Instruments, Sarasota, FL, USA) was used to infuse nanoparticles at a rate of 0.5 μL/min,[25] 10 μL nanoparticles were injected per animal, after which the needle was maintained in the cortex for another 5 min to avoid backflow. Following needle removal, the incision was closed and the animal was allowed to awaken and recover.

HSVtk Survival Studies

After tumor inoculation, mice were randomized and divided into 3 groups (n=10), each group receiving GFP nanoparticles, HSVtk nanoparticles, or sham PBS treatment, respectively. Mice implanted with BT-12 were treated with 447 nanoparticles (90 w/w) while mice implanted with D425 were treated with 537 nanoparticles (90 w/w). Mice received nanoparticle infusions on days indicated in Figure 6 for a total of 3 infusions. All mice received intraperitoneal administration of 50 mg/kg ganciclovir daily on days 10-40 for BT-12 implanted mice and days 7-28 for D425 implanted mice after the first nanoparticle infusion. Animals were monitored daily and assessed for neurological impairment.

Data Analysis and Statistics

All *in vitro* experiments were performed with n=4 unless otherwise noted. Survival data was compiled using the Kaplan-Meier methodology and compared across arms using the Mantel-Cox log-rank test. All statistical tests were performed using the GraphPad Prism6 software.

Results

PBAE nanoparticles enable efficient DNA delivery to AT RT and MB cells in vitro

We synthesized a small library of PBAEs by co-polymerizing small molecule monomers via Michael addition reactions between amines and diacrylates following previously reported protocols (Figure 1A).[26] Briefly, diacrylate “B” monomers were reacted with primary amine-containing “S” monomers (90° C, overnight) to produce acrylate-terminated polymers, which were then end-capped with amine-containing “S” monomers (25°C, 1 hour). The presence of acrylate-terminated polymers following the first step of synthesis was confirmed via ^{1}H NMR with three characteristic acrylate peaks in the 5.5-6.5 ppm range, which disappeared after end-capping reaction (Figure S1). The cationic polymers were mixed with anionic plasmid DNA in acidic buffer to self-assemble into nanoparticles, which were found to be 100-200 nm in diameter with slightly positive surface charges (Figure 1B).

We performed nanoparticle transfection screens on two cell lines established from pediatric patient samples; D425 is a well-characterized Group 3 medulloblastoma cell line,[27] and BT-12 is a highly-cited AT/RT cell line that has been used in pre-clinical studies using HDAC inhibitors, [28] IGF-IR antisense oligonucleotides [29], and neutralizing antibodies [30-31] for exploring treatment.[32-33] Using a GFP reporter plasmid for the initial nanoparticle screen, we found that several PBAE nanoparticle formulations enabled >50% transfection in

both cell lines with minor levels of cytotoxicity (Figure 2). PBAE nanoparticles also enabled significantly higher transfection compared to commercially-available transfection reagents such as 25 kD branched PEI and Lipofectamine 3000™ (Figure 3). Based on our screening results, we chose polymer 1-(3-aminopropyl)-4-methylpiperazine end-capped poly(1,4-butanediol diacrylate-co-4-amino-1-butanol) (447) at a polymer-to-DNA weight-to-weight (w/w) ratio of 90 as the optimal formulation for BT-12 and polymer 1-(3-aminopropyl)-4-methylpiperazine end-capped poly(1,5-pentanediol diacrylate-co-3-amino-1-propanol) (537) at 90 w/w for D425.

We performed nanoparticle uptake experiments in which nanoparticles were formulated to deliver 20% Cy5 labeled DNA, and we characterized nanoparticle uptake in BT-12 cells by assessing intracellular Cy5 fluorescence. Our results showed that 447 90 w/w and 537 90 w/w nanoparticle formulations resulted in the highest levels of cellular uptake as measured by the geometric mean Cy5 fluorescence intensity (Figure 4). These optimized nanoparticle formulations were used for their respective cell lines for the remaining experiments. Uptake pathways leading to transfection were further investigated using an endocytosis pathway inhibition assay in which BT-12 cells were pre-treated with small molecule drugs inhibiting clathrin-mediated endocytosis, lipid raft-mediated endocytosis, caveolin-mediated endocytosis, and macropinocytosis, respectively, before incubation with nanoparticles. Our results demonstrated that polymer end-group structure played an important role in determining the pathway through which nanoparticles were internalized. For example, 446 nanoparticle uptake was significantly inhibited by methyl-β-cyclodextrin (inhibitor of lipid raft-mediated endocytosis), which was not the case for 447 or 537. These studies suggest that for 447 and 537 nanoparticles, the most significant pathway for cellular uptake is caveolin-mediated endocytosis and the cellular uptake pathway that leads to the most efficient transfection is clathrin-mediated endocytosis.

PBAE-HSVtk nanoparticles activate ganciclovir prodrug to induce cell killing in vitro

We next investigated the *in vitro* cell killing capabilities of PBAE nanoparticles encapsulating the HSVtk suicide gene. 447 nanoparticles delivering a plasmid encoding HSVtk or GFP were used to transfect BT-12 cells. Transfected and untransfected controls were replenished with cell culture media containing varying doses of ganciclovir (GCV) on days 1, 3, and 5 post-transfection. Live/dead cell imaging on day 7 post-transfection revealed that GCV treatment in HSVtk transfected cells resulted in >65% cell death at all 3 GCV doses (Figure 5). Similar treatment in GFP-transfected cells did not incur any cytotoxicity, suggesting that cell killing required GCV activation by cells expressing HSVtk. Untransfected cells treated with GCV also did not incur appreciable cytotoxicity, indicating that the GCV doses used did not cause non-specific cell death.

Nanoparticles administered via CED significantly prolong survival in mouse xenograft models in vivo

The robustness of PBAE nanoparticles delivering HSVtk suicide gene therapy was further evaluated in two orthotopic mouse xenograft models, using BT-12 and D425 cells, respectively. Nanoparticles encapsulating either HSVtk or GFP were formulated at the same optimal w/w as *in vitro* experiments and lyophilized with sucrose as a cryoprotectant

following previously published protocols,[10, 24] for ease of storage and to facilitate future manufacturing scalability. To validate our nanoparticle lyophilization procedure, lyophilized nanoparticles were resuspended in water following the same procedure as for *in vivo* injections and characterized using dynamic light scattering. We found that lyophilized nanoparticles were not statistically different in hydrodynamic diameter or zeta potential compared to freshly prepared nanoparticles (Figure S2). Furthermore, lyophilized nanoparticles achieved similar levels of *in vitro* transfection as fresh nanoparticles delivering the same DNA dose, further confirming that lyophilization did not significantly alter nanoparticle properties.

To evaluate *in vivo* nanoparticle efficacy in intracranial tumor models, athymic nude mice were inoculated with 5e5 BT-12 cells or 1.25e5 D425 cells, respectively. Tumors were allowed to form for 7-10 days, after which time nanoparticle treatment began at day 7 for mice implanted with BT-12 cells and day 10 for mice implanted with D425 cells. Each treatment group received 3 nanoparticle infusions through convection-enhanced delivery (CED); mice received 2 μg total DNA dose for each infusion. The first day of treatment was designated as day 0, at which point survival tracking began. Mice also received daily intraperitoneal (i.p.) injections of GCV for the entirety of the treatment period (Figure 6).

In both tumor models, survival of the GFP nanoparticle group closely followed that of the untreated control group, mirroring the results of our *in vitro* cell killing assay. Nanoparticles delivering HSVtk significantly extended survival in both tumor models ($p = 0.0083$ for BT-12 and $p < 0.0001$ for D425, as determined by Mantel-Cox log-rank tests). Mice bearing BT-12 tumors had median survival of 35 days when untreated, and survival was extended to 42 days (20% longer) with HSVtk nanoparticles. D425 tumors were more aggressive, with untreated median survival at 19 days and with HSVtk nanoparticle treatment, median overall survival at 31 days (63% longer) (Figure 6).

Discussion

In this work, we synthesized a small library of poly(beta-amino ester)s (PBAEs) and examined their ability to functionally deliver plasmid DNA encoding a suicide gene to pediatric CNS malignancies. The small size of the nanoparticles (Figure 1) contributed to successful delivery to BT-12 (an AT/RT cell line) and D425 (a MB cell line) *in vitro*. Within the same polymer type, transfection efficacy generally increased with increasing polymer-DNA w/w ratio while cell viability decreased (Figure 2); both phenomenon could be partly explained by the fact that higher polymer doses increase the positive charge of the nanoparticles as well as the number of positively-charged molecules interacting with cells overall, which could simultaneously increase nanoparticle uptake and cytotoxicity by perturbing and disrupting the cellular membrane.[34]

While polymer 447 was equally effective at transfecting both cell lines (45% GFP positive in BT-12 and D425), some polymers were only effective at transfecting one cell line and not the other. For example, 446 enabled transfection exclusively in BT-12 while 457 exclusively transfected D425. To investigate the mechanism by which polymer structure affects transfection efficacy, we studied nanoparticles formulated with polymers 446, 447, and 537

at 90 w/w and their interactions with BT-12 cells. From Figure 2A, we observe that 446 and 447 nanoparticles enabled similar levels of transfection in this cell line while 537 nanoparticles achieved significantly lower transfection levels. Previous studies have reported that molecular weight correlated positively with nanoparticle transfection efficacy in several polymeric nanoparticle systems.[35-36] This was not the case here as polymers 446 and 447 enabled significantly higher transfection than polymer 537 despite having a significantly lower molecular weight (Table S1). The differential transfection levels also do not appear to be dependent on nanoparticle physical characteristics as 447 and 537 nanoparticles do not have statistically significant differences in hydrodynamic diameter or zeta potential (Figure 1).

Previous work suggests that this cell-type specificity may be in part due to the structure of polymer endgroups,[11, 37] which can lead to differential uptake pathways resulting from different nanoparticle-membrane interactions.[38] To test this hypothesis, we performed endocytosis pathway inhibition studies on nanoparticles formulated from polymers 446, 447, and 537. BT-12 cells were pre-treated with small molecule drugs to inhibit specific endocytosis pathways, and nanoparticles were added to cells to study the endocytosis pathways responsible for nanoparticle uptake and DNA transfection (Figure 4B). Compared to polymers end-capped with E7, uptake inhibition of 446 nanoparticles by methyl-β-cyclodextrin was significantly higher, indicating that lipid raft-mediated endocytosis was a major uptake pathway for this polymer structure. Across all three polymer structures, genistein caused very high levels of uptake inhibition without high levels of transfection inhibition, indicating that caveolin-mediated endocytosis was an inefficient endocytosis pathway, through which nanoparticles were taken up, but ultimately not successful for transfection. Chlorpromazine inhibited 60-80% nanoparticle uptake, corresponding to 30-50% transfection inhibition. This indicates that clathrin-mediated endocytosis is a major cellular internalization pathway leading to successful transfection for these polymeric nanoparticles. Taken together, the results demonstrate that subtle changes in PBAE polymer structure can lead to significant changes in the endocytosis and transfection behavior of nanoparticles. Although these correlations are observed, these results do not provide a full explanation for how certain structures lead to higher transfection levels, suggesting that nanoparticle trafficking steps between endocytosis and gene expression, such as endosomal escape, intracellular transport, and nuclear membrane penetration should be further explored to more fully elucidate the mechanisms behind biomaterial-mediated cell type specificity.

Furthermore, while BT-12 cells formed monolayers, D425 cells have been documented to grow as macrospheroids[39] and were transfected in suspension. Our results show that PBAE nanoparticles could be tailored for cell type-specific transfection as well as penetrate and transfect 3D cellular macrospheroids. This data suggest that certain nanomedicine formulations may be potentially useful for pediatric CNS malignancies in general (447 and 537), while other nanomedicine formulations may be able to further improve efficacy for patients with particular tumors (446 and 457). Of note, optimized PBAE formulations significantly outperformed leading commercially-available transfection reagents such as Lipofectamine 3000™.

In vitro assays showed robust and specific cell killing in cells treated with HSVtk nanoparticles and GCV prodrug. GCV treatment alone, with or without nanoparticle-mediated transfection of a reporter gene, did not result in appreciable levels of cytotoxicity. Interestingly, formulation 447 nanoparticles enabled 45% transfection in BT-12 (as assessed via GFP reporter gene screening) but resulted in >65% cell death when used to deliver HSVtk. This is due to a well-documented bystander effect in the HSVtk-GCV system, whereby a fraction of transfected cells can lead to cell death in the greater cell population by releasing activated GCV into the cell medium or through gap junctional intercellular communication.[39] This is an advantage of a suicide gene therapy approach, as the treatment does not rely on 100% transfection efficacy to have a broad effect on a tumor.

In vivo survival studies demonstrated the efficacy of using PBAE nanoparticles carrying HSVtk for treating MB and AT/RT. Of note, the increased median overall survival in mice with AT/RT or MB that were treated with PBAEs carrying HSVtk showed a more impressive therapeutic effect when compared to our previous studies on GBM in rat models.[10] Furthermore, in tumors like MB, which have since been characterized as having one of four possible molecular subtypes,[33] the customizability of PBAE formulations lends itself well to the optimization of personalized nanomedicine technology between these different tumor groups.

It should be noted that PBAEs are not restricted to delivering genes such as HSVtk, as they have been validated as vectors for the delivery of other nucleic acids such as siRNA[19] and miRNA[24] as well. Our data demonstrates proof of principle that PBAEs can be used to deliver genes of interest to MB and AT/RT tumors with significant therapeutic effect. This finding offers a promising alternative avenue to our current limited treatment modalities, with PBAE nanomedicine opening the door to safe and effective non-viral gene-based therapies for pediatric CNS malignancies.

Supplementary Material

Refer to Web version on PubMed Central for supplementary material.

Acknowledgements

The authors would like to thank the NIH (R01CA228133) for support of this work. The authors would also like to thank the Wilmer Equipment Core for use of Cellomics Arrayscan VTI for automated image acquisition and quantification (Microscopy Core Grant EY001765). JC thanks the Johns Hopkins University Deans Research Fund for their fellowship support. YR (DGE-1232825) and DRW (DGE-0707427) thank the NSF for fellowship support, and JK thanks Samsung for scholarship support. JG thanks the Bloomberg~Kimmel Institute for Cancer Immunotherapy for support.

References

1. Gondi V; Yock Tl; Mehta MP. Proton Therapy for Paediatric Cns Tumours—Improving Treatment-Related Outcomes. Nat Rev Neurol 2016; 12:334. [PubMed: 27197578]
2. Smoll NR; Drummond KJ. The Incidence of Medulloblastomas and Primitive Neurectodermal Tumours in Adults and Children. J Clin Neurosci 2012; 19: 1541–1544. [PubMed: 22981874]
3. Biswas A; Kashyap L; Kakkar A; Sarkar C; Julka PK. Atypical Teratoid/Rhabdoid Tumors: Challenges and Search for Solutions. Cancer Manag Res 2016; 8:115. [PubMed: 27695363]

4. Babgi M; Samkari A; Al-Mehdar A; Abdullah S. Atypical Teratoid/Rhabdoid Tumor of the Spinal Cord in a Child: Case Report and Comprehensive Review of the Literature. Pediatr Neurosurg 2018; 53: 254–262. [PubMed: 29788028]
5. Ren Y; Tao C; Wang X; Ju Y. Identification of Rpl5 and Rpl10 as Novel Diagnostic Biomarkers of Atypical Teratoid/Rhabdoid Tumors. Cancer Cell Int 2018; 18: 190. [PubMed: 30479569]
6. Duffner PK; Horowitz ME; Krischer JP; Burger PC; Cohen ME; Sanford RA, et al. The Treatment of Malignant Brain Tumors in Infants and Very Young Children: An Update of the Pediatric Oncology Group Experience. Neuro-Oncology 1999; 1:152–161. [PubMed: 11554387]
7. Tekautz TM; Fuller CE; Blaney S; Fouladi M; Broniscer A; Merchant TE, et al. Atypical Teratoid/Rhabdoid Tumors (Atrt): Improved Survival in Children 3 Years of Age and Older with Radiation Therapy and High-Dose Alkylator-Based Chemotherapy. J Clin Oncol 2005; 23: 1491–1499. [PubMed: 15735125]
8. Dufour C; Beaugrand A; Le Deley MC; Bourdeaut F; André N; Leblond P, et al. Clinicopathologic Prognostic Factors in Childhood Atypical Teratoid and Rhabdoid Tumor of the Central Nervous System: A Multicenter Study. Cancer2012; 118:3812–3821. [PubMed: 22180295]
9. Chi SN; Zimmerman MA; Yao X; Cohen KJ; Burger P; Biegel JA, et al. Intensive Multimodality Treatment for Children with Newly Diagnosed Cns Atypical Teratoid Rhabdoid Tumor. J Clin Oncol 2009; 27: 385. [PubMed: 19064966]
10. Mangraviti A; Tzeng SY; Kozielski KL; Wang Y; Jin Y; Gullotti D, et al. Polymeric Nanoparticles for Nonviral Gene Therapy Extend Brain Tumor Survival in Vivo. ACS Nano 2015; 9: 1236–1249. [PubMed: 25643235]
11. Sunshine J; Green JJ; Mahon KP; Yang F; Eltoukhy AA; Nguyen DN, et al. Small-Molecule End-Groups of Linear Polymer Determine Cell-Type Gene-Delivery Efficacy. Adv Mater 2009; 21: 4947–951. [PubMed: 25165411]
12. Sunshine JC; Sunshine SB; Bhutto; Handa JT; Green JJ. Poly (B-Amino Ester)-Nanoparticle Mediated Transfection of Retinal Pigment Epithelial Cells in Vitro and in Vivo. PloS one 2012; 7: e37543. [PubMed: 22629417]
13. Guerrero-Cázares H; Tzeng SY; Young NP; Abutaleb AO; Quiñones-Hinojosa A; Green JJ. Biodegradable Polymeric Nanoparticles Show High Efficacy and Specificity at DNA Delivery to Human Glioblastoma in Vitro and in Vivo. ACS Nano 2014; 8: 5141–5153. [PubMed: 24766032]
14. Thomas CE; Ehrhardt A; Kay MA. Progress and Problems with the Use of Viral Vectors for Gene Therapy. Nature Reviews Genetics 2003; 4: 346–358.
15. Forbes DC; Peppas NA. Oral Delivery of Small Rna and DNA. J Control Release 2012; 162: 438–445. [PubMed: 22771979]
16. Zhang T; Ma J; Li C; Lin K; Lou F; Jiang H, et al. Core-Shell Lipid Polymer Nanoparticles for Combined Chemo and Gene Therapy of Childhood Head and Neck Cancers. Oncol Rep 2017; 37: 1653–1661. [PubMed: 28098869]
17. Lynn DM; Langer R. Degradable Poly (B-Amino Esters): Synthesis, Characterization, and Self-Assembly with Plasmid DNA. J Am Chem Soc 2000; 122: 10761–10768.
18. Sunshine JC; Peng DY; Green JJ. Uptake and Transfection with Polymeric Nanoparticles Are Dependent on Polymer End-Group Structure, but Largely Independent of Nanoparticle Physical and Chemical Properties. Molecular Pharmaceutics 2012 9: 3375–3383. [PubMed: 22970908]
19. Kozielski KL; Tzeng SY; Hurtado De Mendoza BA; Green JJ. Bioreducible Cationic Polymer-Based Nanoparticles for Efficient and Environmentally Triggered Cytoplasmic Sirna Delivery to Primary Human Brain Cancer Cells. ACS Nano 2014; 8: 3232–3241. [PubMed: 24673565]
20. Tzeng SY; Higgins LJ; Pomper MG; Green JJ. Student Award Winner in the Ph.D. Category for the 2013 Society for Biomaterials Annual Meeting and Exposition, April 10–13, 2013, Boston, Massachusetts: Biomaterial-Mediated Cancer-Specific DNA Delivery to Liver Cell Cultures Using Synthetic Poly (Beta-Amino Ester) S. J Biomed Mater Res A 2013; 101: 1837–1845. [PubMed: 23559534]
21. Zamboni CG; Kozielski KL; Vaughan HJ; Nakata MM; Kim J; Higgins LJ, et al. Polymeric Nanoparticles as Cancer-Specific DNA Delivery Vectors to Human Hepatocellular Carcinoma. J Control Release 2017; 263: 18–28. [PubMed: 28351668]

22. Allard E; Passirani C; Benoit J-P. Convection-Enhanced Delivery of Nanocarriers for the Treatment of Brain Tumors. Biomaterials 2009; 30: 2302–2318. [PubMed: 19168213]
23. Wilson DR; Routkevitch D; Rui Y; Mosenia A; Wahlin KJ; Quinones-Hinojosa A, et al. A Triple-Fluorophore-Labeled Nucleic Acid Ph Nanosensor to Investigate Non-Viral Gene Delivery. Molecular Therapy 2017; 25: 1697–1709. [PubMed: 28479046]
24. Lopez-Bertoni H; Kozielski KL; Rui Y; Lai B; Vaughan; Wilson DR, et al. Bioreducible Polymeric Nanoparticles Containing Multiplexed Cancer Stem Cell Regulating Mirnas Inhibit Glioblastoma Growth and Prolong Survival. Nano Lett 2018; 18: 4086–4094. [PubMed: 29927251]
25. Serwer L; Hashizume R; Ozawa T; James CD. Systemic and Local Drug Delivery for Treating Diseases of the Central Nervous System in Rodent Models. J Vis Exp 2010.
26. Wilson DR; Mosenia A; Suprenant MP; Upadhya R; Routkevitch D; Meyer RA, et al. Continuous Microfluidic Assembly of Biodegradable Poly(Beta-Amino Ester)/DNA Nanoparticles for Enhanced Gene Delivery. J Biomed Mater Res A 2017; 105: 1813–1825. [PubMed: 28177587]
27. Ivanov DP; Coyle B; Walker DA; Grabowska AM. In Vitro Models of Medulloblastoma: Choosing the Right Tool for the Job. J Biotechnol2016; 236:10–25. [PubMed: 27498314]
28. Knipstein JA; Birks DK; Donson AM; Alimova I; Foreman NK; Vibhakar R. Histone Deacetylase Inhibition Decreases Proliferation and Potentiates the Effect of Ionizing Radiation in Atypical Teratoid/Rhabdoid Tumor Cells. Neuro-Oncology 2012; 14: 175–183. [PubMed: 22156471]
29. D'cunja J; Shalaby T; Rivera P; von Büren A; Patti R; Heppner FL, et al. Antisense Treatment of Igf-Ir Induces Apoptosis and Enhances Chemosensitivity in Central Nervous System Atypical Teratoid/Rhabdoid Tumours Cells. Euro J Cancer 2007; 43: 1581–1589.
30. Narendran A; Coppes L; Jayanthan A; Coppes M; Teja B; Bernoux D, et al. Establishment of Atypical-Teratoid/Rhabdoid Tumor (at/Rt) Cell Cultures from Disseminated Csf Cells: A Model to Elucidate Biology and Potential Targeted Therapeutics. J Neuro-Oncol 2008, 90: 171–180.
31. Jayanthan A; Bernoux D; Bose P; Riabowol K; Narendran A.Multi-Tyrosine Kinase Inhibitors in Preclinical Studies for Pediatric Cns at/Rt: Evidence for Synergy with Topoisomerase-I Inhibition. Cancer Cell Int 2011; 11: 44–44. [PubMed: 22206574]
32. Studebaker AW; Hutzen B; Pierson CR; Shaffer TA; Raffel C; Jackson EM. Oncolytic Measles Virus Efficacy in Murine Xenograft Models of Atypical Teratoid Rhabdoid Tumors. Neuro-Oncology 2015; 17:1568–1577. [PubMed: 25838138]
33. Studebaker AW; Hutzen BJ; Pierson CR; Haworth KB; Cripe TP; Jackson EM, et al. Oncolytic Herpes Virus Rrp450 Shows Efficacy in Orthotopic Xenograft Group 3/4 Medulloblastomas and Atypical Teratoid/Rhabdoid Tumors. Mol Ther Oncolytics 2017; 6: 22–30. [PubMed: 28649600]
34. Frohlich E The Role of Surface Charge in Cellular Uptake and Cytotoxicity of Medical Nanoparticles. Int J Nanomedicine 2012; 7: 5577–5591. [PubMed: 23144561]
35. Huang M; Khor E; Lim L-Y. Uptake and Cytotoxicity of Chitosan Molecules and Nanoparticles: Effects of Molecular Weight and Degree of Deacetylation. Pharmaceutical Research 2004; 21: 344–353 [PubMed: 15032318]
36. Eltoukhy AA; Siegwart DJ; Alabi CA; Rajan JS; Langer R; Anderson DG. Effect of Molecular Weight of Amine End-Modified Poly(B-Amino Ester)S on Gene Delivery Efficiency and Toxicity. Biomaterials 2012; 33: 3594–3603. [PubMed: 22341939]
37. Bhise NS; Gray RS; Sunshine JC; Htet S; Ewald AJ; Green JJ. The Relationship between Terminal Functionalization and Molecular Weight of a Gene Delivery Polymer and Transfection Efficacy in Mammary Epithelial 2-D Cultures and 3-D Organotypic Cultures. Biomaterials2010; 31: 8088–8096. [PubMed: 20674001]
38. Kim J; Sunshine JC; Green JJ. Differential Polymer Structure Tunes Mechanism of Cellular Uptake and Transfection Routes of Poly(B-Amino Ester) Polyplexes in Human Breast Cancer Cells. Bioconjugate Chemistry 2014; 25: 43–51. [PubMed: 24320687]
39. Wikstrand CJ; Friedman HS; Bigner DD. Medulloblastoma Cell-Substrate Interaction in Vitro. Invasion Metastasis 1991; 11: 310–324. [PubMed: 1822845]

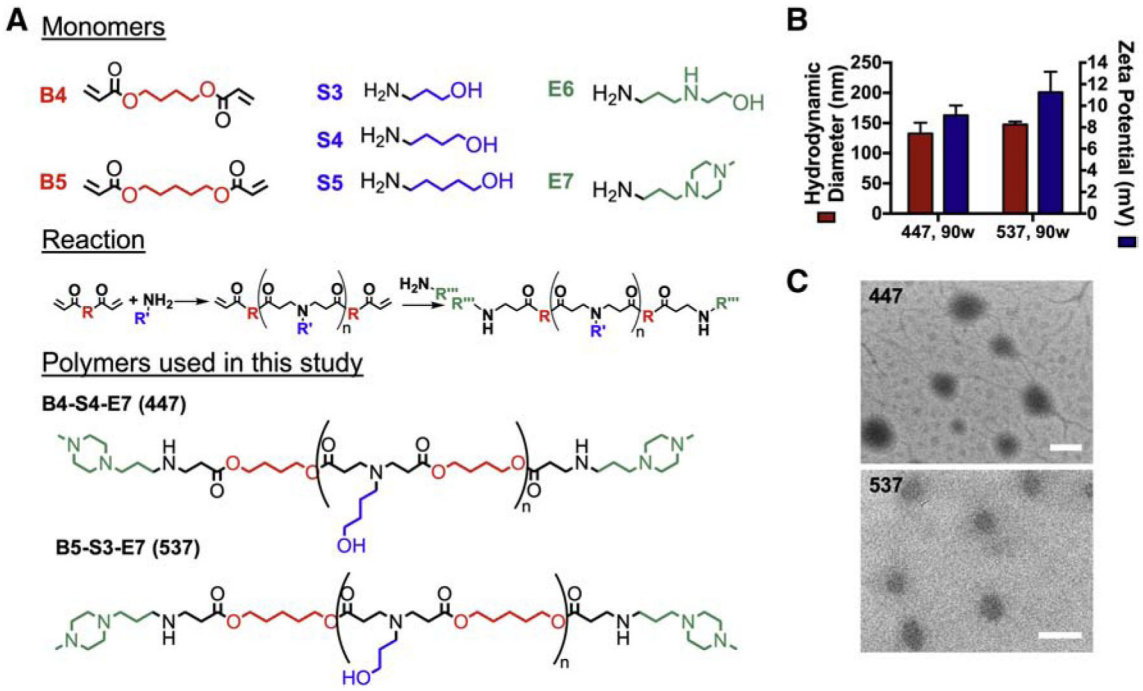

Figure 1. PBAE chemical structures and nanoparticle characteristics.

(A) PBAEs are synthesized from B, S, and E monomers via Michael addition reactions. Structures of top polymers used in this study are shown. **(B)** Hydrodynamic diameter and zeta potential measurements of top nanoparticle formulations as measured by dynamic light scattering, n = 3. **(C)** Representative TEM images of 447 and 537 nanoparticles, respectively; scale bar = 200 nm.

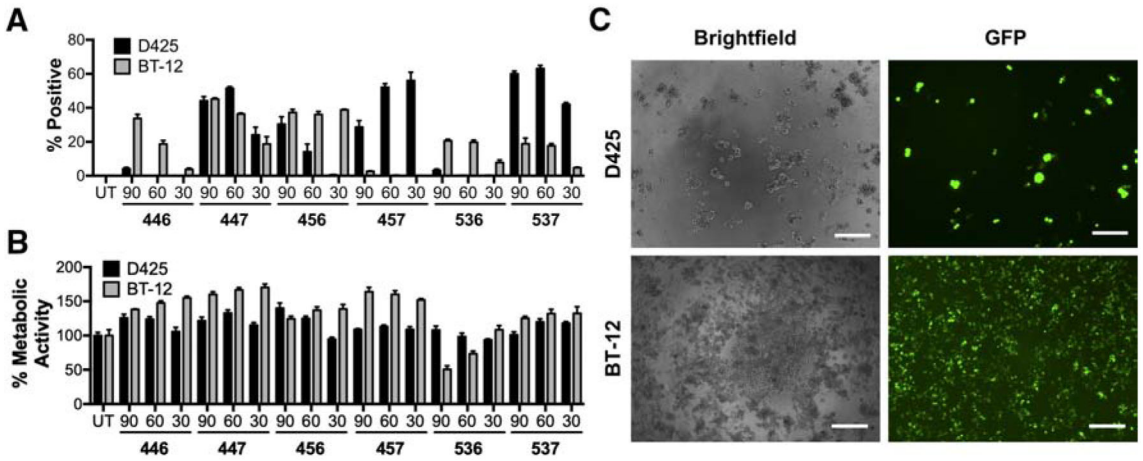

Figure 2. ***In vitro*** **nanoparticle screening in D425 and BT-12 cells.**

Transfection efficacy shown as percent GFP positive cells **(A)** and **(B)** metabolic activity after treatment with different nanoparticle formulations; n = 4. **(C)** Fluorescence microscopy images of both cell lines transfected with their respective optimal nanoparticle formulations (537, 90 w/w for D425; 447, 90 w/w for BT-12); scale bar = 200 μm.

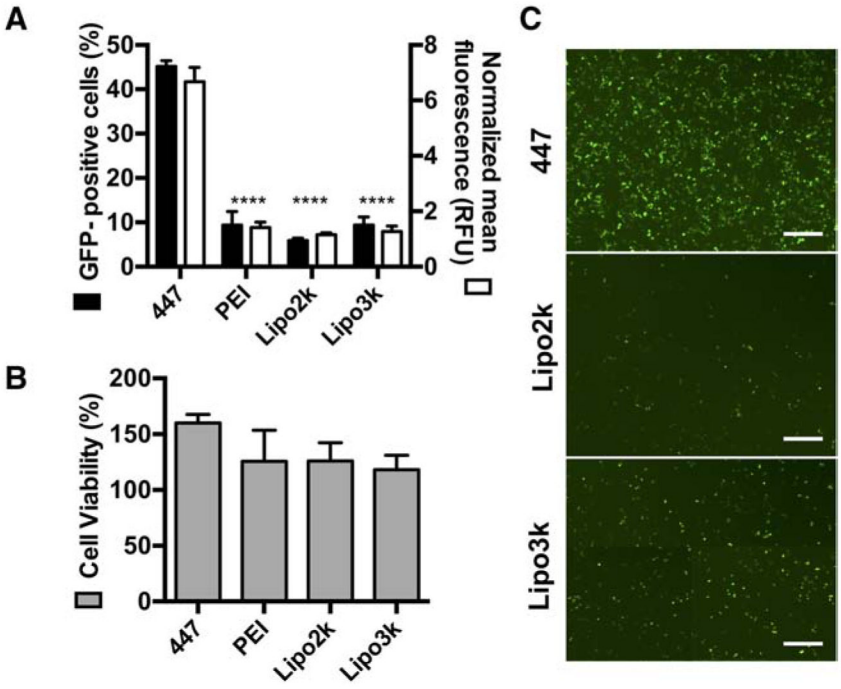

Figure 3. PBAE nanoparticles enable higher transfection than commercially-available transfection reagents.

(A) Formulation 447 nanoparticles enabled significantly higher transfection in BT-12 cells compared to 3 commercially-available transfection reagents; statistical significance assessed by ordinary one-way ANOVA Dunnett's multiple comparisons test (n = 4; ****$p<0.001$). **(B)** Nanoparticles caused negligible levels of cytotoxicity; metabolic activity/cell viability measured by MTS assay and normalized to non-transfected control (n = 4). **(C)** Fluorescence microscopy images of cells transfected with different reagents; scale bar = 200 μm.

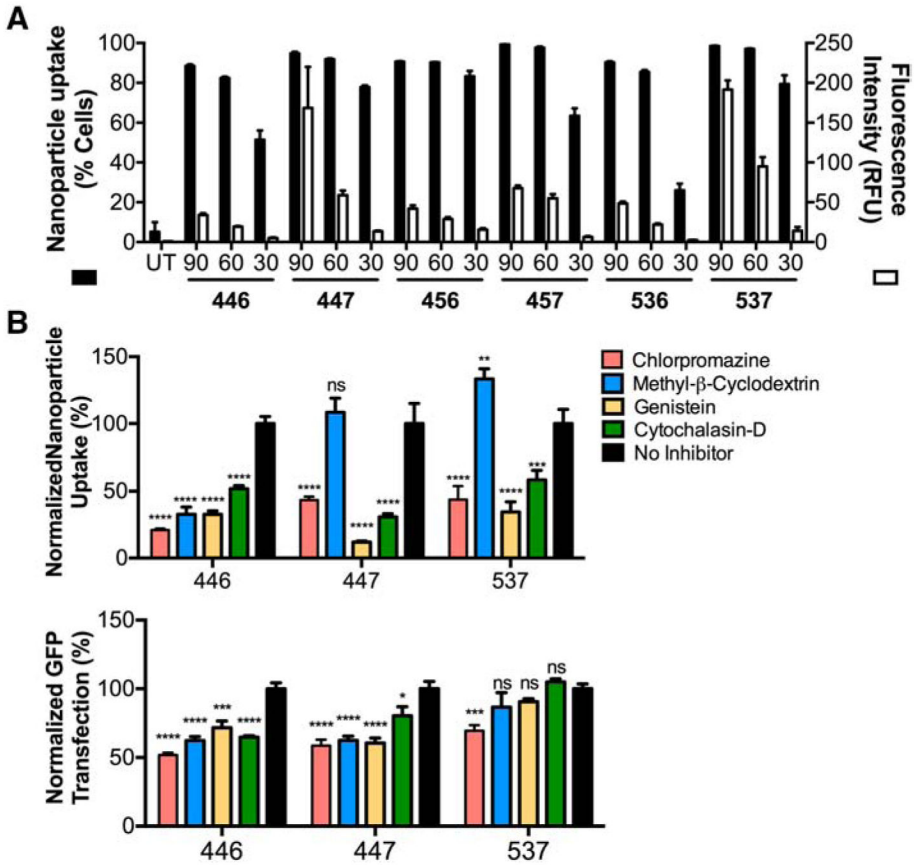

Figure 4: Effect of endocytosis pathway on nanoparticle uptake and transfection.

(A) Cellular uptake of nanoparticles encapsulating Cy5-labled DNA. Nanoparticle uptake is expressed as the percentage of cells containing Cy5 signal as well as the geometric mean Cy5 fluorescence intensity (n = 4). **(B)** Uptake (top) and transfection (bottom) of select polymers (all nanoparticles were formulated at 90 w/w) after endocytosis pathway inhibition (n = 4). Chlorpromazine was used to inhibit clathrin-mediated endocytosis; methyl-β-cyclodextrin – lipid raft-mediated endocytosis; genistein – caveolin-mediated endocytosis, and cytochalasin-D – macropinocytosis. Uptake and transfection are expressed as the fluorescence intensity of each inhibitor-treated condition normalized to the no inhibitor group. Statistical significance was determined using 2-way ANOVA with Dunnett's multiple comparisons test as compared to the no inhibitor group for each polymer (*$p \leq 0.05$, **$p \leq 0.01$, ***$p \leq 0.001$, **** $p \leq 0.0001$.)

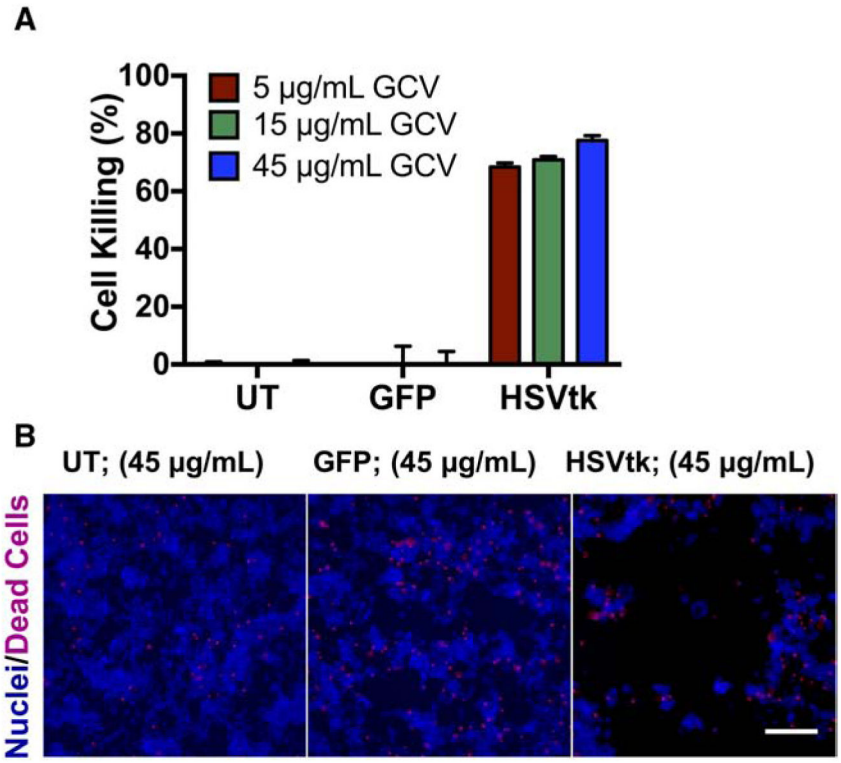

Figure 5. PBAE nanoparticles delivering HSVtk enables cell killing *in vitro*.

(A) BT-12 cells were transfected with nanoparticles encapsulating either GFP or HSVtk plasmid DNA (447, 90 w/w, 600 ng/well), and only cells transfected with HSVtk showed high levels of cell death upon GCV treatment. Un-transfected cells (UT) were treated with GC V only as negative control. (n = 4). **(B)** Fluorescence microscopy images of BT-12 cells treated with indicated nanoparticle formulations at 45 μg/mL GCV 7 days post-transfection. Cells were stained with Hoechst 33342 nuclear dye (blue) or propidium iodide for dead cells (magenta). Scale bar =100 μm.

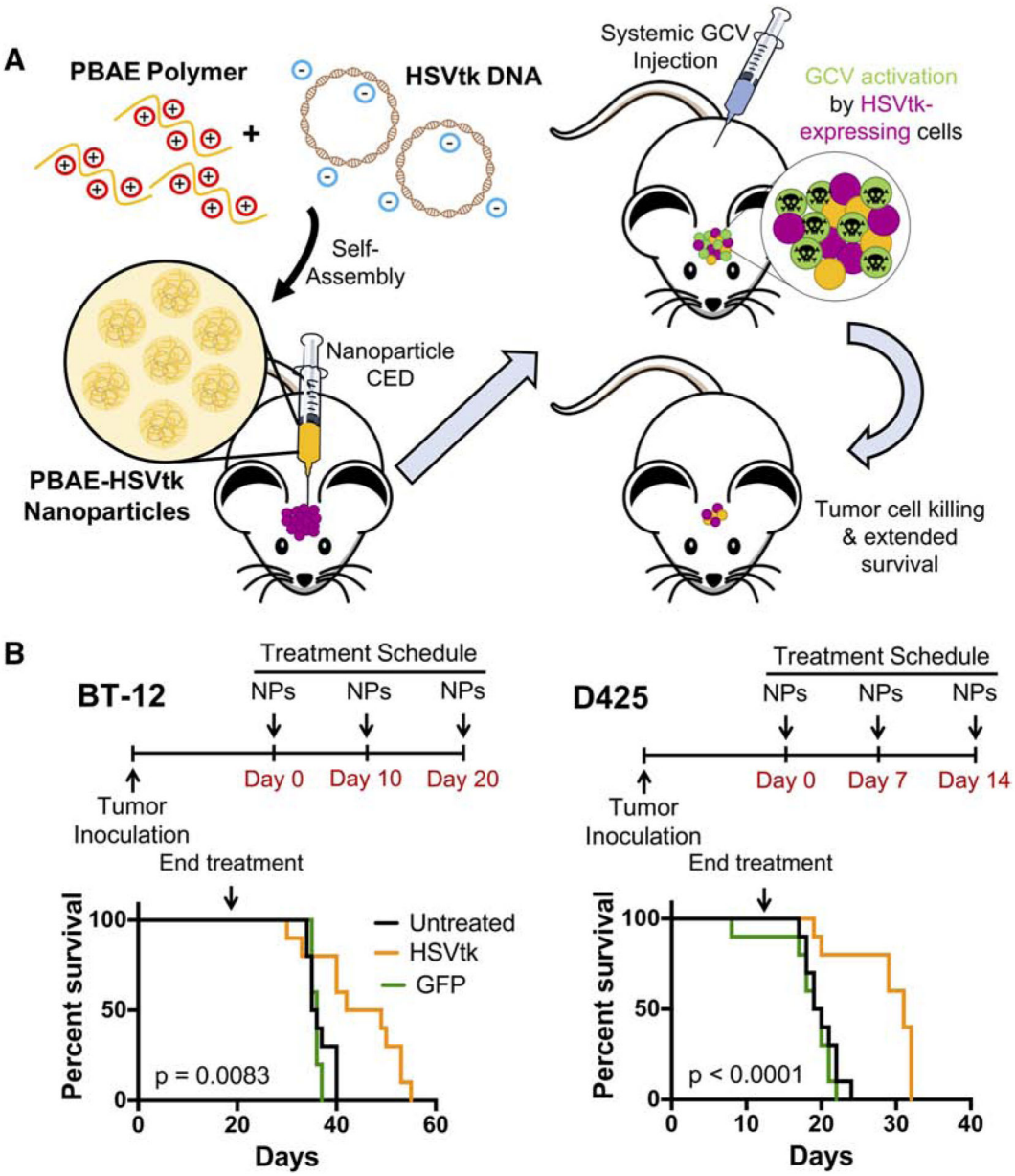

Figure 6. Convection-enhanced delivery of PBAE nanoparticles significantly extended survival in mouse orthotopic xenograft models *in vivo*.

(A) Schematic of *in vivo* study: PBAEs self-assembled into nanoparticles with plasmid DNA, which were infused intratumorally via CED; mice also received intraperitoneal injections of GCV prodrug, which were activated in transfected cells, leading to tumor cell killing and extended survival. **(B)** Treatment schedule and Kaplan-Meier survival curves for each tumor model; n= 10 animals per group.